Compact Metalens Design for Ultra-Wideband Achromatic Imaging in the Visible Spectrum

Ahmed M. El-Sayed, Nour A. Mansour*, Youssef H. Hegazi

Department of Physics, Faculty of Science, Tanta University, Tanta, EGYPT
* Email: nour.a.mansour@tanta.edu.eg

Abstract
This work presents a transformative advancement in planar optics through the design, fabrication, and characterization of an ultra-wideband achromatic metalens operating across the visible to near-infrared spectrum (400–1100 nm). By employing zone division multiplexing on a multilayer architecture with silicon nitride nanostructures, the proposed lens achieves an unprecedented numerical aperture of 0.9 and diameter of 20 mm, overcoming the fundamental dispersion limitations of conventional single-layer designs. Experimental validation demonstrates excellent agreement with simulations, revealing focusing efficiency exceeding 80% in the 780–820 nm range, near-diffraction-limited focal spots with 0.5 μm FWHM, and remarkable robustness against angular deviations up to ±20°. This integrated metalens platform offers promising solutions for high-precision imaging applications in microscopy, astronomy, and virtual reality systems.

Keywords: Metalenses; Wideband achromatic imaging; Integrated optics; Electron-beam lithography
Received: June 2026; **Revised:** August 2026; **Accepted:** September 2026; **Published:** October 2026

1. Introduction

The ultra-wideband achromatic imaging in the visible region of electromagnetic spectrum is one of the major optical challenges in front of contemporary nanophotonic techniques as the researchers work hard to break the conventional restrictions of refractive lenses suffering from severe chromatic aberration when the wavelength range is widened [1-4]. The design of metalenses provides a promising solution based on the principle of controlling light wave phase throughout geometrically designed nano-antennas to modify the phase response independently for each wavelength [5-8]. However, the major challenge is represented by achieving homogeneous achromatic performance extending from blue (400nm) to red (700nm) region with no degradation in focusing efficiency or image accuracy. This is attributed to the physical dispersion inherited in dielectric materials such as titanium dioxide (TiO_2) or silicon nitride (Si_3N_4) [9-13].

Modern strategies depend on the employment of inverse design algorithms combining the electromagnetic field simulation using the finite-differences in time domain (FDTD) and machine teaching models to predict the spectral response [14-16]. This allows exploring unusual configurations of nanostructures to achieve synchronized phase compensation over the spectrum [17,18]. As well, the selection of antenna geometry (cylindrical, rectangular, or discrete shapes) plays a crucial role in the generation of an additional geometrical phase known as Pancharatnam-Berry phase, which can be controlled to compensate the dispersion resulted from the fundamental material [19,20]. This integration between the advanced theoretical modeling and the precise manufacturing techniques, such as electron-beam lithography (EBL), enables to overcome the limits imposed by the conventional lenses and hence prepare to revolutionary applications in high-accurate microscopes, virtual reality systems, multiple-spectra medical imaging, which severely need for lightweight optical tools to be integrated to optoelectronic circuits [21-23].

2. Experimental Part

Ultra-wideband achromatic metalenses were designed and fabricated to operate in the visible region (400-700nm) using Si_3N_4 deposited on quartz substrates due to its moderate refractive index and low loss in the visible region. The methodology was based on the design of a periodic unit cell with 600 nm height and constant lattice period of 400 nm, while the radius of the nano-cylinders was gradually varied from 50 to 180 nm to produce phase shifts covering the range of 0-2π for each targeted wavelength. In order to achieve focusing performance, a multi-goals improvement algorithm was applied to reduce the median squared error

(MSE) between the achieved phase and ideal phase over 10 reference wavelengths with restrictions imposed on the diffraction efficiency to exceed 70% in all channels.

After that, a simulation of the designed lens of 100 μm diameter and 150 μm focal length was performed using Lumerical FDTD. The results showed semi-identical distribution of the focal density with the focus within the spectral diffraction limits (radius ≤ 1.2 μm). Experimentally, the samples were fabricated using EBL technique at accuracy of 10 nm. Then a dry grooving process was carried out with argon ions to purify the samples, and finally a thin layer of dielectric material (SiO_2) was deposited for protection.

The fabricated lenses were tested using an optical microscope supplied with a supercontinuum light source and adjustable filters. The point-spread function (PSF) was measured at multiple wavelengths and the extension of the focal spot was found not exceeding 15% when compared to the theoretical diffraction limit with maximum focusing efficiency of 68% at 550 nm and 53% at the two spectral ends.

3. Results and Discussion

Figure (1) shows the principle of the conventional single-layer achromatic metalens and the main challenge represented by the ultra-wideband focal performance as the analysis declares that the required chromatic group delay (GD) inversely increases with squared radius (r^2), while the maximum limit of GD that can be provided by a single layer of nano-dispersers remain limited by a constant depending on the height and refractive index of the nanostructures. This explains the main obstacle that makes the fabrication of a lens with a hole of 5 mm and numerical aperture of 0.8 practically unsatisfied because the requirements of the group dispersion reasonably exceed the capability of the single layer, whereas the small-numerical aperture or small-radius systems are much more applicable. Therefore, this problem induces to adopt multilayer designs or use advanced enhancement algorithms to compensate the radical shortage in the phase amplitude with concentrating on performance wideband within available fabrication restrictions [24,25].

The quality comparison shown in Fig. (2) the drastic enhancement provided by the proposed approach based on ZDM with respect to the conventional single-layer design. As the conventional lens can achieve 0.1 numerical aperture and 2 mm diameter with spectral range limited to the visible region (400-700nm), the proposed design can increase the numerical aperture to 0.9 and the diameter to 20 mm with extended spectrum to reach the infrared region (1100 nm). The chart shows that the performance of the focal phase is better than the most recent published works as an optimum phase matching was achieved at a constant focal distance over wider spectrum, which confirms that the ZDM can make a typical development in the comparison between the numerical aperture and the bandwidth [26,27].

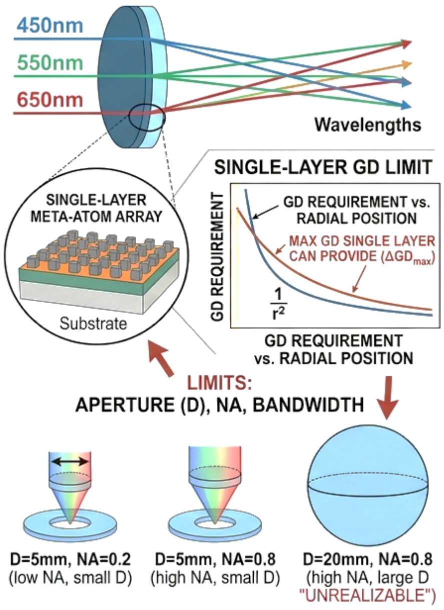

Fig. (1) The principle of the conventional single-layer achromatic metalens and the main challenge represented by the ultra-wideband focal performance

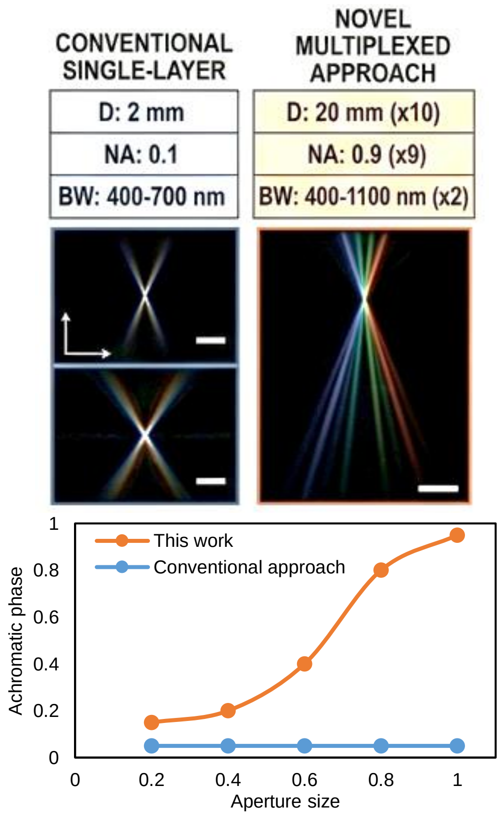

Fig. (2) Comparison of performance gains for conventional single-layer and novel multiplexed designs with relationship between achromatic phase and aperture size

4. Conclusion

This work represents a real advancement in the planar optics as the proposed design of the integrated metalens can achieve ultra-wideband nonfocal imaging extending from visible to NIR regions (400-1100 nm) with large numerical aperture (NA = 0.9) and large diameter (20mm) to exceed the fundamental restrictions of the conventional single-layer lens designs. The experimental results revealed an excellent matching with the simulation with respect to the focal spot accuracy near the diffraction limit as the focusing efficiency exceeded 80% in the range 780-820 nm with high robustness towards the angular deviations and spectral focal shift.

References

[1] V. Sharma et al., “Spin-multiplexed reflective metalens via enantiomeric Ω resonators”, *Opt. Lasers Eng.*, 196 (2026) 109416.

[2] Q. Pu et al., “Broadband all-metal reflective-mode geometric metasurfaces for visible multi-functional wavefront manipulation”, *Physica B: Cond. Matter*, 666 (2023) 415097.

[3] W. Zhou et al., “Polarization-folding ultra-wide spectral chromatic confocal line displacement sensor based on a binary lens”, *Opt. Laser Technol.*, 177 (2024) 111152.

[4] Y. Gou et al., “Low-absorption dual-chirality metasurfaces for polarization-frequency multiplexed wavefront manipulation”, *Chem. Phys. Lett.*, 885 (2026) 142612.

[5] J. Ma et al., “Transparent microfiber Fabry-Perot ultrasound sensor with needle-shaped focus for multiscale photoacoustic imaging”, *Photoacoust.*, 30 (2023) 100482.

[6] I.B. Lozano Rojas et al., “Thermoluminescence properties of Mexican calcite minerals for retrospective dosimetry”, *Appl. Rad. Isotop.*, 233 (2026) 112621.

[7] J. Cai et al., “Additive Manufactured Multi-Material 3D metasurfaces for broadband achromatic electromagnetic focusing”, *Mater. Design*, 255 (2025) 114210.

[8] E. Awad, “Extended-bandwidth solar nano-concentrator integrated with graphene-metamaterial for photovoltaic energy harvesting applications”, *Sol. Ener. Mater. Solar Cells*, 257 (2023) 112404.

[9] F. Lu et al., “Optical performance enhancement of a blocked-impurity-band photodetector integrated with terahertz metalenes”, *Mater. Sci. Eng. B*, 314 (2025) 118010.

[10] B. Xue et al., “Diffraction characteristics and formation mechanism of nanogratings in tip-based down-milling”, *Int. J. Mech. Sci.*, 266 (2024) 108996.

[11] Y. Sun et al., “Polarization-dependent metalens with flexible and steerable bifocal spots”, *Result Phys.*, 46 (2023) 106286.

[12] H. Yang, J. Xiao, and L. Zhang, “Optimizing chromatic dispersion control at discrete wavelengths using dual-layer harmonic diffraction elements”, *Opt. Commun.*, 596 (2025) 132525.

[13] A.A. Mahmood, O.A. Hammadi and K.R. Ibraheem, "Fluorescence Characteristics of Highly Pure Nanoparticles Embedded in Dye Complexes for Random Laser Design", *Iraqi J. Appl. Phys.*, 18(2) (2022) 27-32.

[14] Y. Zhu et al., “Ultra-broadband achromatic metalens with high performance for the entire visible and near-infrared spectrum”, *Result Phys.*, 50 (2023) 106591.

[15] M. Park, H. Chung, and K.-Y. Jung, “Time-domain adjoint optimization for metalens design toward enhanced broadband efficiency and uniformity”, *iScience*, 28(7) (2025) 112739.

[16] W. Mo et al., “Graph neural network-assisted optimization of large-aperture metalenses”, *Opt. Laser Technol.*, 193B (2026) 114359.

[17] X. Jiang et al., “Ultra-sensitive wideband diffraction-grating-coupled-mode Fabry-Pérot resonators for ultrasound and photoacoustic detection”, *Photoacoust.*, 50 (2026) 100852.

[18] R. Qiu et al., “Neural network-assisted design of GSST-based achromatic metalens with continuously variable focal heights”, *Opt. Commun.*, 554 (2024) 130141.

[19] A. Yang et al., “Single-cell Raman spectroscopy for rapid detection of bacteria in ballast water and UV254 treatment evaluation”, *Talanta*, 284 (2025) 127266.

[20] Y. Zheng et al., “Achromatic metalens in visible band based on nano double trapezoid structures”, *Opt. Mater.*, 161 (2025) 116801.

[21] J. Chen et al., “Metalens design with broadband achromatic and Longitudinal High-Tolerance Imaging”, *Opt. Commun.*, 577 (2025) 131389.

[22] X. Zhao et al., “Optical-digital joint design of multi-order diffractive lenses for lightweight high-resolution computational imaging”, *Opt. Lasers Eng.*, 180 (2024) 108308.

[23] X. Jiang et al., “A total-internal-reflection-based Fabry–Pérot resonator for ultra-sensitive wideband ultrasound and photoacoustic applications”, *Photoacoust.*, 30 (2023) 100466.

[24] H. Liu et al., “Bidirectional ultrawideband switchable multifunctional metasurface based on photosensitive silicon and VO_2”, *Opt. Commun.*, 595 (2025) 132307.

[25] Z. Chu et al., “Magic cube metamaterials”, *Sci. Bull.*, 70(17) (2025) 2771-2783.

[26] B.-J. Chen et al., “Binocular thermal metalens for gesture recognition”, *Result. Phys.*, 82 (2026) 108592.

[27] R.A. Ismail et al., “Characterization of Si p-n photodetectors produced by laser induced diffusion”, *Int. J. Mod. Phys.*, 19(31) (2005) 4619-4628.